Perfluorooctane sulfonic acid, a persistent organic pollutant, inhibits iodide accumulation by thyroid follicular cells in vitro

Perfluorooctane sulfonic acid, a persistent organic pollutant, inhibits iodide accumulation by thyroid follicular cells *in vitro*

Amalia Conti [a], Chiara Strazzeri [b], and Kerry J. Rhoden [c]

[a] Department of Medical and Surgical Sciences (DIMEC), University of Bologna, S. Orsola-Malpighi Hospital, via Massarenti 9, Bologna 40138, Italy; amalia.conti2@unibo.it

[b] Department of Medical and Surgical Sciences (DIMEC), University of Bologna, S. Orsola-Malpighi Hospital, via Massarenti 9, Bologna 40138, Italy; chiara.strazzeri@studio.unibo.it

[c] Department of Medical and Surgical Sciences (DIMEC), Health Sciences & Technologies Interdepartmental Center for Industrial Research (CIRI SDV), University of Bologna, S. Orsola-Malpighi Hospital, via Massarenti 9, Bologna 40138, Italy; kerry.rhoden@unibo.it

Corresponding author

Kerry J. Rhoden, UO Genetica Medica, Policlinico S. Orsola-Malpighi pad 11, via Massarenti 9, Bologna 40138, Italy; kerry.rhoden@unibo.it

Declarations of interest: none

Abstract

Poly- and perfluoroalkyl substances (PFAS) are a class of endocrine disrupting chemicals (EDCs) reported to alter thyroid function. Iodide uptake by thyroid follicular cells, an early step in the synthesis of thyroid hormones, is a potential target for thyroid disruption by EDCs. The aim of the present study was to evaluate the acute effects of perfluorooctane sulfonic acid (PFOS) and perfluorooctane carboxylic acid (PFOA), two of the most abundant PFAS in the environment, on iodide transport by thyroid follicular cells *in vitro*. Dynamic changes in intracellular iodide concentration were monitored by live cell imaging using YFP-H148Q/I152, a genetically encoded fluorescent iodide biosensor. PFOS, but not PFOA, acutely and reversibly inhibited iodide accumulation by FRTL-5 thyrocytes, as well as by HEK-293 cells transiently expressing the Sodium Iodide Symporter (NIS). PFOS prevented NIS-mediated iodide uptake and reduced intracellular iodide concentration in iodide-containing cells, mimicking the effect of the NIS inhibitor perchlorate. PFOS did not affect iodide efflux from thyroid cells. The results of this study suggest that disruption of iodide homeostasis in thyroid cells may be a potential mechanism for anti-thyroid health effects of PFOS. The study also confirms the utility of the YFP-H148Q/I152 cell-based assay to screen environmental PFAS, and other EDCs, for anti-thyroid activity.

Key words: endocrine chemical disruptor, thyroid follicular cell, iodide, Sodium Iodide Symporter, poly- and perfluoroalkyl substances (PFAS), perfluorooctane sulfonic acid (PFOS)

1. Introduction

Per- and polyfluoroalkyl substances (PFAS) are a group of man-made chemicals that have raised world-wide concern as persistent organic pollutants that threaten ecosystems and human health (ITRC, 2018; Wang et al., 2017). Thanks to their unique physicochemical properties - resistance to oil, water, heat and degradation - PFAS have been extensively used in manufacturing processes since the 1950's. They are present in a vast array of industrial and consumer products, including fire-fighting foams, hydraulic systems, electronic components, building materials, paints, textiles, food packaging, non-stick cookware, cleaning agents and cosmetics, among others. At least 3000 PFAS are on the global market (KEMI, 2015), of which perfluorooctane sulfonic acid (PFOS) and perfluorooctanoic acid (PFOA) have historically been the most widely used.

The same physicochemical properties that underlie their industrial and consumer utility have also led to the ubiquitous and persistent occurrence of PFAS in the environment and biota. PFAS are bioaccumulated thanks to their ability to interact with both phospholipids and proteins (Ng and Hungerbühler, 2014). Partitioning to cell membranes, and noncovalent binding to transporters and serum proteins, accounts for the broad tissue distribution of PFAS in wildlife and man, and to their slow elimination from the body (Ng and Hungerbühler, 2014). Indeed, PFOS and PFOA have extremely long serum elimination half-lives in man of 4.8 and 3.5 years, respectively (Olsen et al., 2007).

Human exposure to PFAS has been linked to a variety of health effects, including altered hormone and cholesterol levels, impaired pre- and post-natal development, reproductive dysfunction, immunotoxicity, liver damage, and certain types of cancer (EFSA, 2018; USEPA, 2016). The World Health Organization has included both PFOS and PFOA in its assessment of endocrine disrupting chemicals (EDCs) (WHO, 2013). Epidemiologic and laboratory studies have reported thyroid disruption by both compounds, although not

consistently (Coperchini et al., 2017; EFSA, 2018; USEPA, 2016). Reported effects are highly heterogeneous, and may involve different steps in the synthesis, metabolism, clearance and action of thyroid hormones. Given that PFAS and PFOA exist in the environment in their anionic form, it is reasonable to hypothesize that, in the body, these chemicals may interfere with the homeostasis of physiological anions, and in the case of the thyroid gland, with that of iodide.

Iodine is necessary for the synthesis of thyroid hormones, thyroxine (T4) and triiodothyronine (T3). The thyroid gland concentrates circulating iodide thanks to the Sodium Iodide Symporter (NIS; SLC5A5), a secondary active transporter present on the basolateral surface of thyroid follicular cells (Portulano et al., 2014). Iodide uptake by NIS is followed by diffusion across the apical membrane into the lumen of thyroid follicles for incorporation into thyroglobulin, the precursor of thyroid hormones. Using a high throughput screening assay, the U.S. EPA's Endocrine Disruptor Screening Program (EDSP) identified PFOS as a NIS inhibitor in HEK293T cells expressing human NIS and FRTL-5 thyroid cells (Buckalew et al., 2020; Wang et al., 2019, 2018). The aim of the present study was to evaluate the effect of PFOS and PFOA on intracellular iodide concentration in thyroid cells *in vitro* in order to address impairment of iodide homeostasis as a potential mechanism for the anti-thyroid effect of PFAS.

2. Materials and Methods

2.1. Materials

Chemicals and reagents, unless otherwise specified, were obtained from Sigma-Aldrich, including PFOS (catalog #77283) and PFOA (catalog # 71468). Cell culture media, unless otherwise specified, were obtained from Euroclone (Italy). FRTL-5 cells were kindly provided by Dr. F. Curcio and Dr. F.S. Ambesi-Impiombato of the University of Udine (Italy). Plasmids pcDNA3.1-YFP-H148Q/I152L (Galietta et al., 2001) and pcDNA3-hNIS (Smanik et al., 1996) were kindly provided by Dr. LGV Galietta (TIGEM, Italy) and Dr. S.M. Jhiang (Ohio State University), respectively. Other materials and their sources are described in the relevant Methods section.

2.2. Cell culture and transfection

FRTL-5 normal rat thyroid follicular cells were cultured in Coon's modified nutrient mixture F-12 Ham (Sigma-Aldrich) supplemented with 5% newborn calf serum, 1 mg/ml insulin, 3.6 ng/ml hydrocortisone, 5 mg/ml apotransferrin, 10 ng/ml gly-his-lys acetate, 10 ng/ml somatostatin, 1 mU/ml thyroid-stimulating hormone (TSH), 100 U/ml penicillin and 100 mg/ml streptomycin (Ambesi-Impiombato et al., 1980). HEK-293 cells were cultured in Dulbecco's modified Eagle medium (DMEM) supplemented with 10% fetal bovine serum (FBS), 2 mM glutamine, 100 U/ml penicillin and 100 mg/ml streptomycin. All cells were maintained at 37^{o}C in humidified air containing 5% CO2.

A clonal population of FRTL-5 cells with stable expression of YFP-H148Q/I152L (referred to hereafter as FRTL5-YFP) was previously generated and used to monitor intracellule iodide (Rhoden et al., 2008, 2007). HEK-293 cells were transiently co-transfected with pcDNA3.1-YFP-H148Q/I152L and pcDNA3-hNIS, using Lipofectamine 3000 (ThermoFisher Scientific) according to manufacturer's instructions. Transfection efficiency,

111 estimated as the proportion of fluorescent cells 48h post-transfection, was typically >80%.
112 hNIS expression in HEK-293 cells was confirmed by Western blotting using anti-
113 hNIS(KELE) antibody.

114 **2.3. Dynamic monitoring of intracellular iodide concentration**

115 Intracellular iodide concentration was monitored by microscopic live cell imaging with YFP-
116 H148Q/I152L, a fluorescent genetically-encoded iodide biosensor, as previously described
117 (Cianchetta et al., 2010; Di Bernardo et al., 2011; Rhoden et al., 2007, 2008). Cells were
118 sub-cultured on 25 mm diameter round glass coverslips in 6-well culture dishes.
119 Coverslips were mounted on a thermostatically-controlled RC-21BR imaging chamber
120 connected to a VC-8 perfusion valve control system and TC-344B temperature controller
121 (Warner Instruments). Fluorescence intensity (excitation 500±12.5 nm, emission 545±17.5
122 nm) was monitored with an Axiovert 200 inverted fluorescence microscope (Carl Zeiss)
123 equipped with a 40x oil immersion objective and Lambda 10C optical filter changer (Sutter
124 Instrument Company; Crisel Instruments, Rome, Italy). Image acquisition was performed
125 with a Coolsnap HQ^2 CCD (Photometrics; Crisel Instruments, Rome, Italy) and Metafluor
126 Imaging Software (Molecular Devices; Crisel Instruments, Rome, Italy). Images were
127 acquired with an exposure of 25 ms every 10 seconds.

128 Imaging chambers were perfused continuously with a serum-free balanced salt solution
129 (BSS) composed of 137 mM NaCl, 2.7 mM KCl, 0.7 mM $CaCl_2$, 1.1 mM $MgCl_2$, 1.5 mM
130 KH_2PO_4, 8.1 mM Na_2HPO_4 and 10 mM glucose (pH 7.4) at 37^{o}C. Baseline fluorescence
131 was recorded for at least 5 min at the beginning of each experiment, after which cells were
132 exposed to 10 μM NaI in order to induce iodide accumulation. The effects of test reagents
133 (PFOS, PFOA, $NaClO_4$, or ouabain) on intracellular iodide concentration were evaluated
134 according to one or more of the following protocols: Protocol I, 2 min pre-treatment +/- test

reagents, followed by 10 min exposure to 10 μM NaI +/- test reagents; Protocol II, 10 min exposure to 10 μM NaI, followed by 10 min exposure to 10 μM NaI +/- test reagents; Protocol III, 10 min exposure to 10 μM NaI, followed by 10 min exposure to BSS +/- test reagents. Stock solutions of test reagents were prepared in distilled water and diluted appropriately in BSS.

Intracellular iodide concentration was quantified from iodide-induced changes in cellular YFP-H148Q/I152L fluorescence, as described previously (Cianchetta et al., 2010; Di Bernardo et al., 2011; Rhoden et al., 2008, 2007). Average fluorescence intensity was quantified within a region-of-interest (ROI) containing 20-50 cells, paying careful attention to select an ROI without cell loss during the entire duration of the experiment. Background fluorescence of a cell-free area was subtracted. To control for the decline in cellular fluorescence over time due to photo-bleaching of the fluorophore, baseline fluorescence in iodide-free BSS measured during the first 5 min of each experiment, was fit by non-linear regression to a one-phase exponential decay curve. Cellular fluorescence (F) at each time point of the experiment was then normalized to the corresponding best-fit value of baseline fluorescence (F_0) to obtain a measure of relative fluorescence ($RF=F/F_0$). Intracellular iodide concentration was calculated according to the equation $[I^-] = K_{0.5}(RF_{max}–RF)/(RF-RF_{min})$ where $K_{0.5}$ is the affinity of YFP-H148Q/I152L for iodide, RF is relative fluorescence at each time point during the experiment, and RF_{max} and RF_{min} represent the maximal and minimal values of RF in the absence and presence of saturating iodide, respectively. RF_{max} is 1, by definition, and mean values for RF_{min} (0.036) and $K_{0.5}$ (1.372 mM) were determined experimentally using FRTL5-YFP cellular extracts (see section 2.4). The maximal rate of iodide uptake, defined as the maximal rate of change of intracellular iodide concentration ($\Delta[I^-]/\Delta t$), was estimated by fitting intracellular $[I^-]$ to a one-phase exponential association equation with respect to time, and obtaining the derivative of the best fit curve.

160 The rate constant of iodide efflux was estimated by fitting intracellular [I^-] to a one-phase
161 exponential decay equation with respect to time.

162 **2.4. YFP-H148Q/I152L fluorescence in cellular extracts**

163 In order to evaluate whether PFAS interfere with the ability of YFP-H148Q/I152L to detect
164 iodide, experiments we carried out using FRTL5-YFP cellular extracts. Cells were cultured
165 in T75 flasks till near confluence, detached in PBS and micro-centrifuged at 12000g for 10
166 min at 4^{o}C. Cellular pellets were disrupted with a pestle in 10 mM HEPES pH 7 (200 μl per
167 pellet) and passed repeatedly through a 28-gauge needle. Lysates were centrifuged, and
168 supernatants containing liberated YFP-H148Q/I152L were collected on ice. Pellets were
169 re-suspended in 10 mM HEPES pH 7, homogenized and centrifuged to recover further
170 YFP-H148Q/I152L. Samples of pooled supernatants were diluted 1:1 with HEPES 10 mM
171 pH 7 containing NaI and/or PFOS to achieve a range of final concentrations (0.1-100 mM
172 NaI, 0.1-10 mM PFOS). Replicate 10 μl aliquots were deposited on a coverslip, and
173 fluorescence images were acquired with the same imaging station used for cellular
174 experiments. Average fluorescence intensity within a constant ROI was quantified and
175 normalized against the mean value obtained in the absence of NaI, to obtain a measure of
176 relative fluorescence ($RF=F/F_0$). The affinity of YFP-H148Q/I152L for iodide ($K_{0.5}$) was
177 defined as the concentration of NaI causing a 50% of maximal decrease in relative
178 fluorescence intensity.

179 **2.5. SDS-PAGE electrophoresis and Western blotting**

180 Cells were lysed in ice-cold buffer (50 mM Tris pH 7.4, 150 mM NaCl, 0.1% SDS, 1 %
181 Triton-X, 1 mM EDTA), supplemented with Roche cOmplete Protease Inhibitor cocktail.
182 Lysates were passed repeatedly through a 20-gauge needle on ice. Protein concentration
183 was measured colorimetrically using the DC Protein Assay (Bio-Rad) according to the

manufacturer's instructions. Lysates were mixed 1:1 with a modified Laemmli sample buffer (125 mM Tris pH 6.8, 20% glycerol, 20% SDS 20%, 200 mM dithiothreitol, and 0.2% bromophenol blue), and incubated for 30 min at 37°C. Samples (40 μg protein) were subjected to SDS-PAGE electrophoresis using hand-cast 9% gels in a Mini-Protean Tetra Vertical Electrophoresis Cell (Bio-Rad). Samples were transferred onto 0.2 μM nitrocellulose membranes using the Trans-Blot Turbo Transfer System (Bio-Rad). For Western blotting, membranes were incubated with WesternBreeze Blocker/Diluent (ThermoFisher) for 1h at room temperature, primary antibody overnight at 4°C, and peroxidase-conjugated secondary antibody for 1h at room temperature, with frequent washing in Tris-buffered saline containing 0,1% Tween. Bound antibodies were detected by enhanced chemiluminescence using WESTAR Supernova substrates (Cyanagen, Bologna, Italy) and a ChemiDoc™ XRS+ Imaging System (Bio-Rad). The following antibodies were used: rabbit polyclonal anti-hNIS(KELE) antibody (Tazebay et al., 2000) generously provided by Dr. N. Carrasco (Yale University) and Dr. C. Portulano (formerly of Albert Einstein College of Medicine, USA), mouse monoclonal anti-γ-tubulin antibody clone GTU-88 (Sigma-Aldrich), goat anti-rabbit IgG-peroxidase antibody (Sigma-Aldrich), and goat anti-mouse IgG-peroxidase (Sigma-Aldrich).

2.6. Cytotoxicity

Cell viability was assessed using a Quick Cell Proliferation Colorimetric Assay Kit Plus (BioVision) based on the cleavage of water-soluble tetrazolium salt to formazan by cellular mitochondrial dehydrogenase. FRTL-5 cells were exposed to PFOS or PFOA (1-100 μM) for 1h, and viability was assayed according to manufacturer's instructions. Absorbance was read at 450 nm using a Model 680 Microplate Reader (Bio-Rad).

2.7. Data analysis

Data analysis, including curve fitting, iodide quantification and statistical analyses, were performed using Graphpad Prism Software. Data are expressed as mean values +/- SEM of *n* independent experiments performed on cells from different passages. Concentration-response data were fit by non-linear regression to a four-parameter logistic equation. PFOS potency was expressed as the half-maximal inhibitory concentration (IC_{50}). Statistical differences between treatment groups were determined by ANOVA followed by Dunnett's multiple comparison tests.

3. Results

3.1. Effects of PFOS and PFOA on iodide accumulation in FRTL-5 thyroid cells

YFP-H148Q/I152L was used as an iodide biosensor in FRTL-5 thyroid cells. To exclude the possibility that PFOS may interfere with the fluorophore's ability to detect iodide, its effect on YFP-H148Q/I152L fluorescence was first measured in a cellular extract following lysis of FTRL5-YFP cells. PFOS (100 μM) had no effect on the fluorescence intensity of FRTL5-YFP extracts, nor did it alter the sensitivity of YFP-H148Q/I152L to NaI ($K_{0.5}$ = 1.3 vs. 1.0 mM in the absence and presence of PFOS respectively, n=4) (Figure 1A). Higher concentrations of PFOS than those used for functional studies (1-10 mM) reduced the fluorescence of FRTL5-YFP extracts, suggesting a direct interaction of PFOS with the fluorophore at such high concentrations (Figure 1 B).

Perfusion of intact FRTL5-YFP cells with 10 μM NaI resulted in a rapid decline in cellular fluorescence that was both reversible and reproducible over time (Figure 1 C). We have previously demonstrated this response to be due to cellular uptake of iodide via the transporter NIS (Rhoden et al., 2007). The response to NaI was diminished in the presence of 1 or 10 μM PFOS but was fully restored following removal of PFOS from the perfusate (Figure 1 C). Baseline cellular fluorescence was not affected by PFOS, nor was cellular morphology altered from the beginning to the end of experiments lasting up to 1 h. A higher concentration of PFOS (100 μM) caused some cells (<10%) to detach from coverslips during a 10 min exposure period.

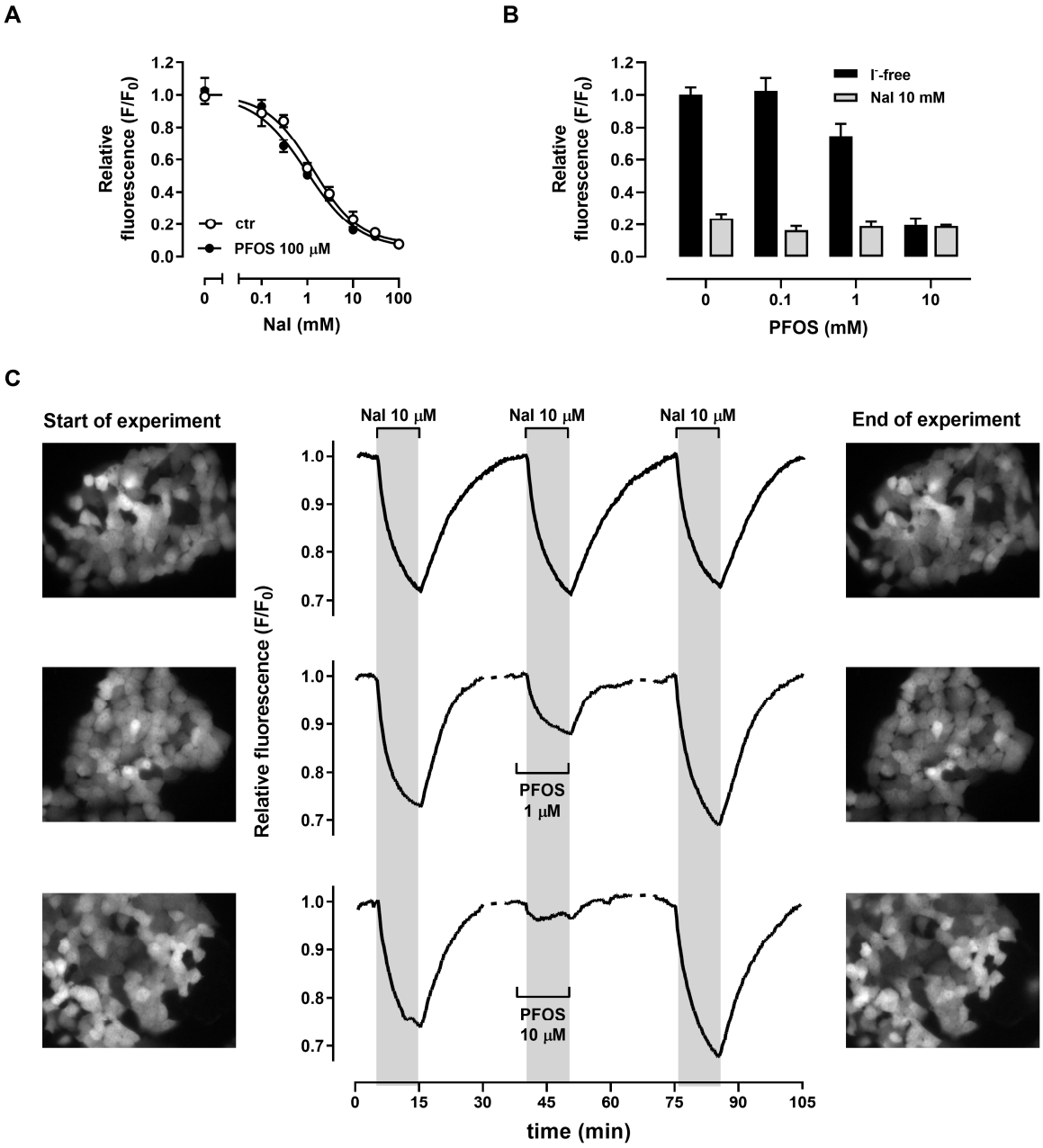

Figure 1. Effect of PFOS on YFP-H148Q/I152L fluorescence of FRTL5-YFP cells. (A) Fluorescence intensity of cellular extracts in the absence/presence of 100 μM PFOS and 0.1-100 mM NaI. (B) Fluorescence intensity of cellular extracts in the absence/presence of 10 mM NaI and 0.1-10 mM PFOS. (C) Representative tracings of YFP-H148Q/I152L fluorescence in living cells exposed to NaI and PFOS, and corresponding images captured at the beginning (left) and end (right) of each experiment. Repeated exposure of cells to 10 μM NaI induced reproducible changes in fluorescence intensity (upper tracing), with recovery of resting fluorescence between each exposure. NaI-induced fluorescence changes were reduced in the presence of 1 μM PFOS (middle tracing) or 10 μM PFOS (lower tracing) and were restored following PFOS washout. Symbols and bars in A and B represent mean ± SEM of n=4 replicates.

Intracellular iodide concentration in FRTL5-YFP cells was estimated from NaI-induced changes fluorescence intensity. Consistent with the known ability of NIS to concentrate iodide within thyroid cells (Portulano et al., 2014), exposure to 10 μM NaI resulted in a rapid increase in intracellular iodide concentration, reaching close to 500 μM within 10 min (Figure 2 A). PFOS (0.1-100 μM), added 2 min before and during NaI perfusion (Protocol I), caused a concentration-dependent decrease in iodide uptake (Figure 2 A-C). The concentration-dependence of PFOS obeyed a log sigmoidal relationship relative to both the maximal rate of iodide uptake (max $\Delta[I^-]/\Delta t$) and the concentration of intracellular iodide reached after 10 min of perfusion with NaI ($[I^-]_{10min}$). Thus, PFOS inhibited iodide uptake with an IC_{50} value of 1.0 μM (log IC_{50} -5.99 +/- 0.20) and Hill slope of -0.99 for $\Delta[I^-]/\Delta t$, and an IC_{50} value of 0.65 μM (log IC_{50} -6.19 +/- 0.16) and Hill slope of -0.96 for $[I^-]_{10min}$ (n=6-9). The lowest concentration of PFOS causing a detectable decrease in intracellular iodide concentration was 0.3 μM or 150 ng/ml ($p<0.05$ Dunnett's multiple comparison test versus no PFOS control). At the highest concentration used (100 μM or 50 μg/ml), PFOS caused a near-complete (>95%) inhibition of iodide uptake, as did the NIS inhibitor $NaClO_4$ (Figure 2 D-F). In contrast, PFOA (100 μM, 41 μg/ml) had no significant effect on iodide uptake (Figure 2 D-F).

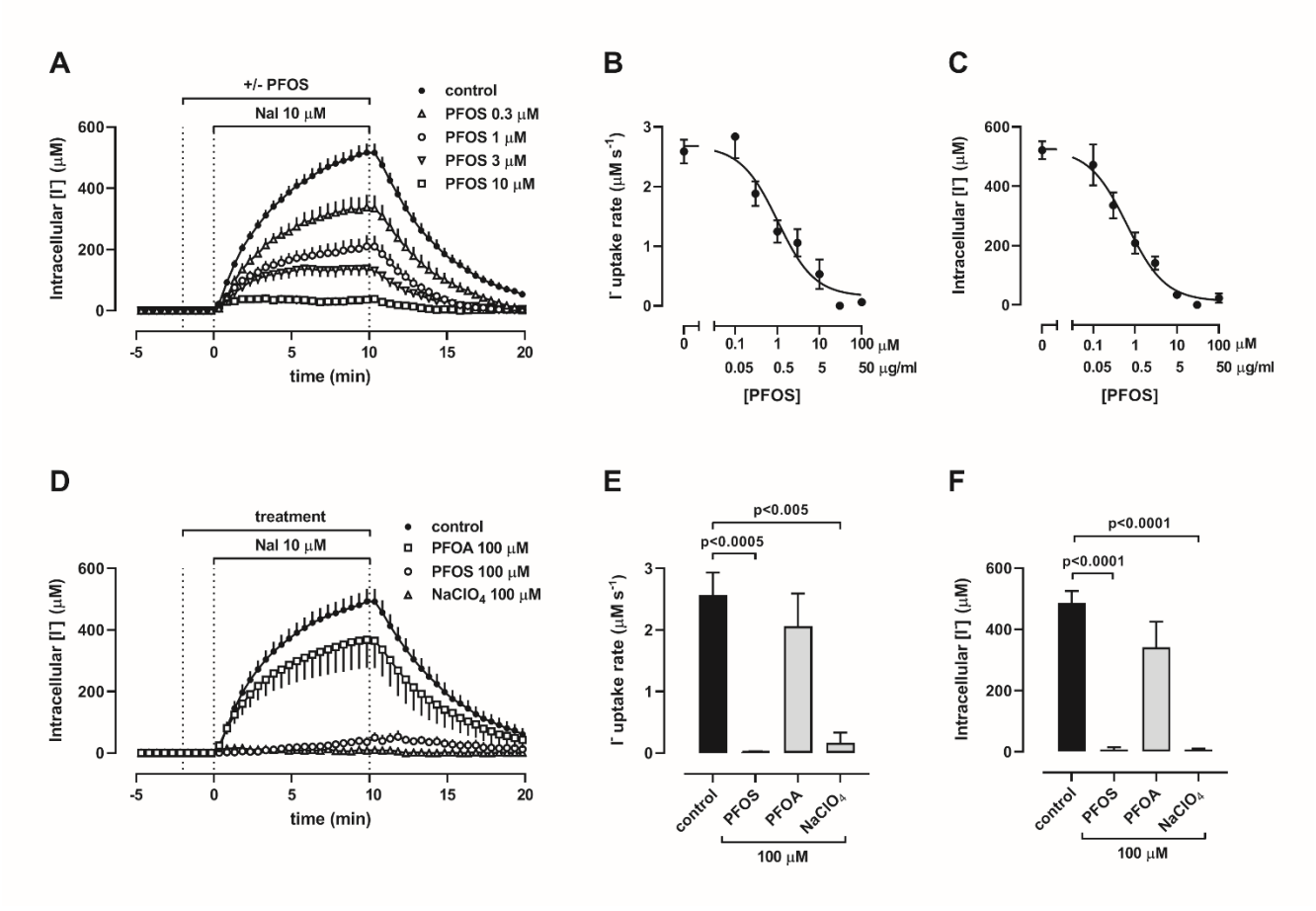

Figure 2. PFOS, but not PFOA, decreases iodide uptake by FRTL5-YFP cells. Cells were exposed to PFOS, PFOA or $NaClO_4$, added 2 min before and during exposure to 10 μM NaI for a further 10 min. Graphs A-C show the effects of PFOS (0.1-100 μM) on (A) the time-course of iodide uptake, (B) the maximal rate of iodide uptake, and (C) the intracellular iodide concentration at t=10 min. Graphs D-E show the effects of 100 μM PFOS, PFOA or $NaClO_4$ on (D) the time-course of iodide uptake, (E) the maximal rate of iodide uptake, and (F) the intracellular iodide concentration at t=10 min. Symbols and bars represent mean ± SEM of n=6-9 experiments.

PFOS was also able to reduce iodide concentration in iodide-containing FRT5-YFP cells, evidenced as a reversal of NaI-induced fluorescence changes (Figure 3 A). In this case, cells were first exposed to 10 μM NaI for 10 min to pre-load them with iodide, followed by PFOS in the continued presence of NaI for a further 10 min (Protocol II). To control for differences in iodide uptake between replicate experiments that could mask the effect of PFOS, intracellular iodide concentration in each experiment was normalized to the level reached after 10 min of iodide uptake, immediately before PFOS addition (i.e. $[I^-]_{10min}$ is defined as 100%). PFOS caused a time- and concentration-dependent decrease in iodide concentration (Figures 3 B-C), with an IC_{50} of 0.92 μM (log IC_{50} -6.04 +/- 0.14) and Hill slope of -0.94 (n=4-8). The effect of PFOS (100 μM) mimicked that of $NaClO_4$ (100 μM), whereas PFOA (100 μM) had no significant effect (Figures 3 D-E).

To determine whether altered sodium gradients could contribute to PFOS-induced responses, the effect of the Na-K ATPase inhibitor ouabain (100 μM) on intracellular iodide concentration was also examined (Protocol II). Compared to the time control, ouabain reduced intracellular iodide concentration in iodide-containing cells by only 23% (figure 4 A), in contrast to the 82% inhibition induced by 10 μM PFOS over the same 10 min time frame (from figure 3 B).

To determine whether PFOS stimulates iodide efflux, FRTL5-YFP cells were exposed to 10 μM NaI for 10 min to pre-load them with iodide, followed by washout in NaI-free BSS with or without 10 μM PFOS (Protocol III). Intracellular iodide concentration decreased upon NaI-removal with a similar rate constant in the presence (0.014+0.001 s^{-1}) and absence (0.012+0.002 s^{-1}) of PFOS (figure 4 B).

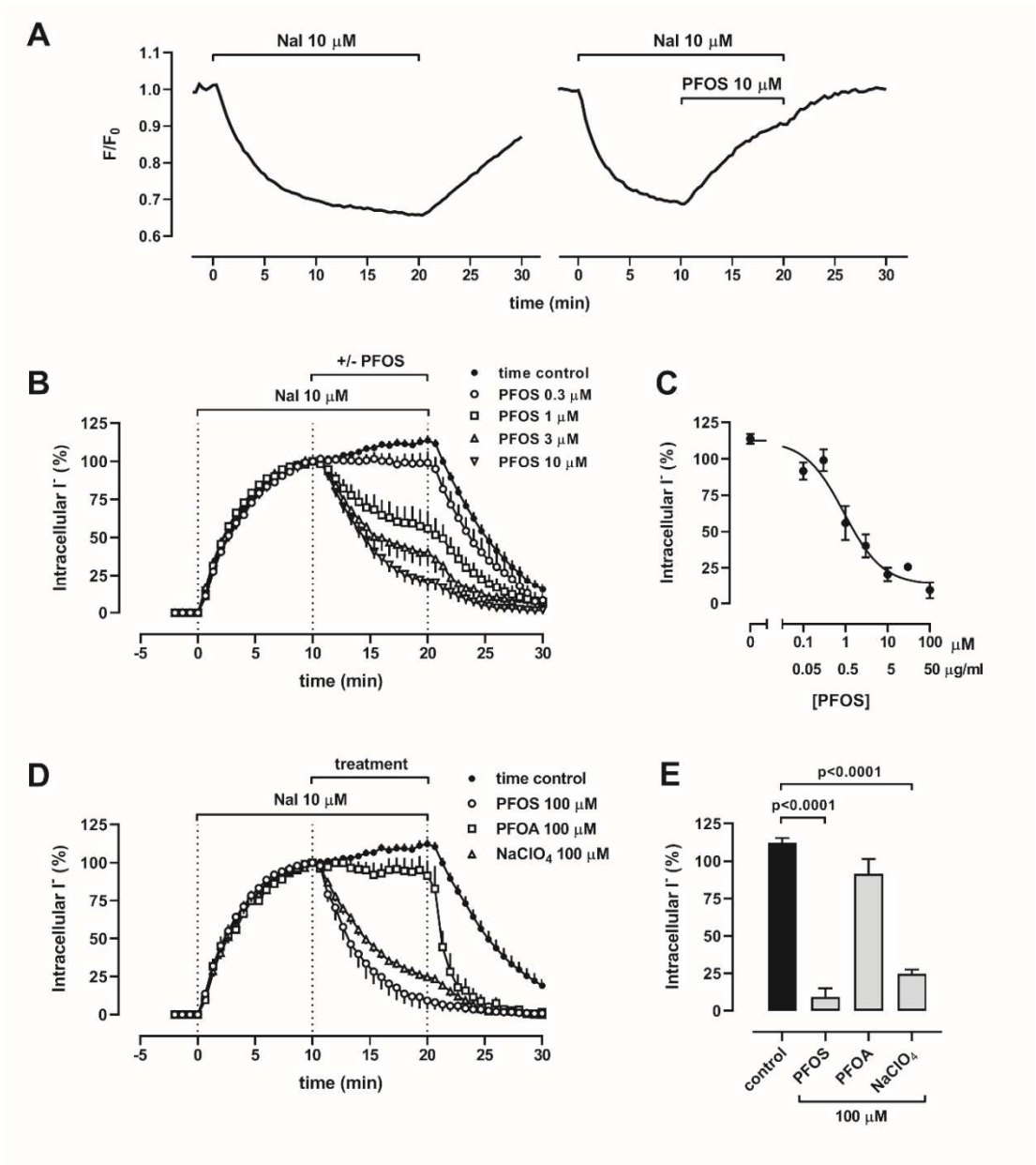

Figure 3. PFOS, but not PFOA, decreases iodide concentration in iodide-containing FRTL5-YFP cells. Cells were exposed to 10 μM NaI for 10 min, followed by 10 μM NaI +/- PFOS, PFOA or $NaClO_4$ for a further 10 min. (A) Representative tracing of normalized YFP-H148Q/I152L fluorescence (F/F_0). (B) Time-dependent changes in intracellular iodide concentration induced by 0-10 μM PFOS. (C) PFOS concentration-dependence of intracellular iodide concentration measured at t=20 min. (D) Time-dependent changes in intracellular iodide concentration induced by 100 μM PFOS, PFOA or $NaClO_4$. (E) Effect of 100 μM PFOS, PFOA and $NaClO_4$ on intracellular iodide concentration measured at t=20 min. In graphs B-E, intracellular iodide concentration was normalized within each individual experiment to the level reached after 10 min of uptake, before the addition of test agents. Symbols and bars represent mean ± SEM of n=4-8 experiments.

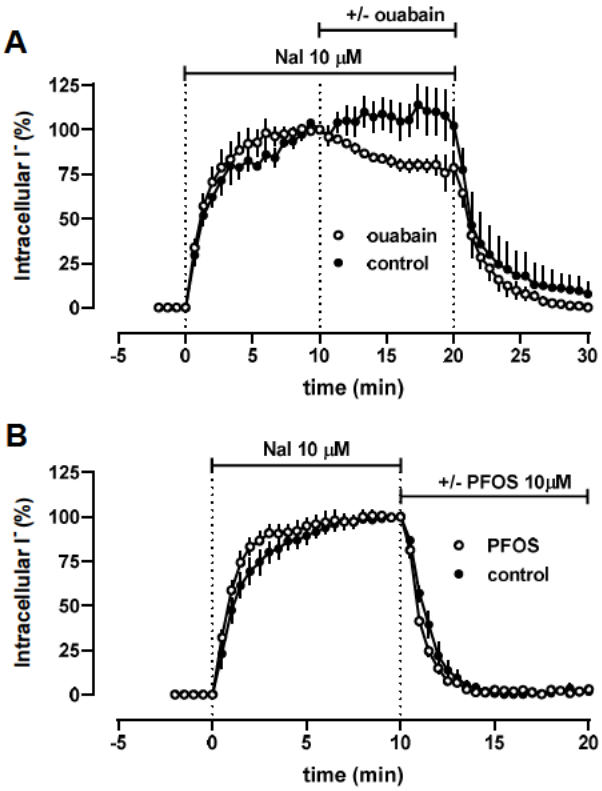

Figure 4. Effect of ouabain and PFOS on intracellular iodide concentration in FRTL5-YFP cells. (A) Cells were exposed to 10 µM NaI for 10 min, followed by 10 µM NaI +/- 100 µM ouabain for a further 10 min. (B) Cells were exposed to 10 µM NaI for 10 min, followed by NaI-free BSS +/- 10 µM PFOS for a further 10 min. Intracellular iodide concentration was normalized within each individual experiment to the level reached after 10 min of uptake, before the addition of test agents Symbols and bars represent mean ± SEM of n=4 experiments.

3.2. Effect of PFOS on iodide accumulation in HEK-293 expressing hNIS

hNIS expression in HEK-293 cells transfected with hNIS cDNA was confirmed by Western blotting (Figure 5 A). NaI (10 μM) decreased the cellular fluorescence of HEK293-YFP-hNIS cells by 25% over 10 min but had a neglible (<2%) effect on HEK293-YFP cells, consistent with NIS-mediated iodide uptake in the former (Figure 5 B). PFOS (10 μM) did not alter baseline fluorescence in either cell model, but reduced fluorescence changes induced by NaI in HEK293-YFP-hNIS cells. This effect was reversible, with full recovery of NaI-induced responses following washing with physiological solution. PFOS (10 μM) also provoked the loss of iodide from iodide-containing HEK293-YFP-hNIS cells, as indicated by the reversal of NaI-induced fluorescence changes. Quantitation of intracellular iodide (Figure 5 C-D) revealed a significant inhibition of iodide uptake by 10 μM but not 1 μM PFOS, in terms of both the maximal rate of iodide uptake and the near steady-state concentration reached after 10 min exposure to NaI.

3.3 Effect of PFOS and PFOA on cell viability

Cell viability of FRTL-5 cells exposed to 1-100 μM PFOS or PFOA for 1h was assessed using a tetrazolium-based assay (Figure 6). Although one-way ANOVA indicated an overall difference ($p<0.05$) for both compounds, Dunnett's multiple comparisons post-tests failed to reveal any significant differences in the viability of cells exposed to either compound compared to the time control. Tukey's multiple comparison test only revealed a significant decrease in the viability of cells exposed to 100 μM versus 30 μM PFOS ($p<0.05$).

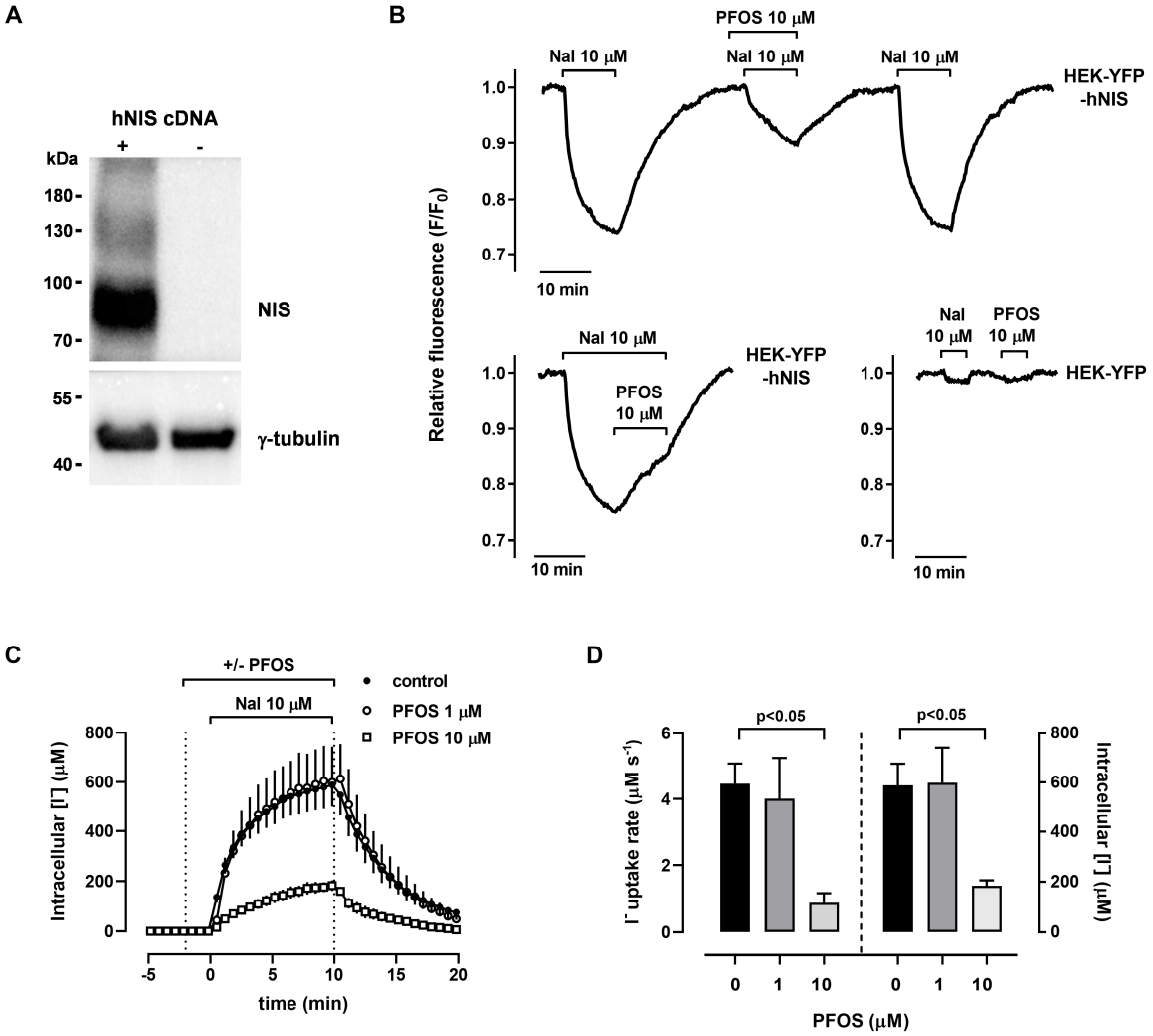

Figure 5. PFOS decreases iodide accumulation by HEK293 cells expressing hNIS. (A) Western blot detection of hNIS and γ-tubulin (loading control) in HEK-293 cell lysates (40 μg protein), 48h after transfection with/without hNIS cDNA. (B) Representative tracings of normalized YFP-H148Q/I152L fluorescence (F/F_0) in HEK293-YFP-hNIS and HEK293-YFP cells exposed to 10 μM NaI and/or 10 μM PFOS. (C) Time course of iodide uptake in HEK293-YFP-hNIS in the presence of 0, 1, or 10 μM PFOS. (D) Effect of PFOS on the maximal rate of iodide uptake and intracellular iodide concentration at t=10 min in HEK293-YFP-hNIS cells. Symbols and bars represent mean ± SEM of n=4 experiments.

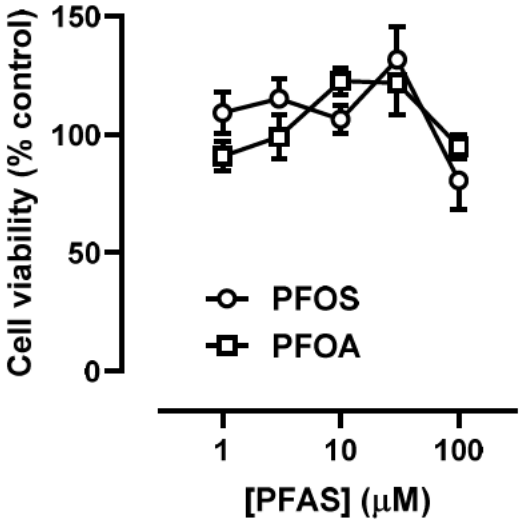

Figure 6. Effect of PFOS and PFOA on cell viability in FRTL.5 cells. Cells were exposed to PFOS or PFOA for 1 h, after which cell viability was measured with a tetrazolium-based assay. Symbols and bars represent mean ± SEM of n=3-4 replicates.

4. Discussion

Cell-based assays are useful tools to investigate the mechanisms by which environmental contaminants disrupt physiological processes. Current screening assays for NIS inhibitors include radiotracer and chemical assays (Hallinger et al., 2017; Lecat-Guillet et al., 2007; Waltz et al., 2010), both of which provide end-point measurements of iodide uptake by NIS-expressing cells. In this study, we used a genetically encoded halide-sensitive biosensor, YFP-H148Q/I152L, to monitor intracellular iodide concentration by live cell imaging (Rhoden et al., 2008, 2007). Iodide quenching of cellular YFP-H148Q/I152L fluorescence is rapid, reversible, and concentration-dependent. The assay requires small numbers of cells and can be used to follow the time course of iodide influx and efflux in a single experiment. Cells can be repeatedly exposed to extracellular iodide, with reproducible changes in YFP-H148Q/I152L fluorescence. Although the technique suffers some limitations (e.g. interference by intracellular pH, not suitable for difficult-to-transfect cells), it is particularly useful to study the disruption of iodide homeostasis by EDCs.

The results of this study demonstrate that PFOS inhibits NIS-mediated iodide accumulation in thyroid follicular cells, as well as in non-thyroid cells with heterologous NIS expression. PFOS mimicked the NIS inhibitor perchlorate in its ability to both prevent iodide uptake by cells and reduce iodide concentration in iodide-containing cells. In the intact thyroid gland, the polarized expression of transport proteins on follicular cells – NIS on the basolateral surface, pendrin, anoctamin-1 and possibly other channels on the apical surface – normally ensures the unidirectional flow of iodide towards the follicular lumen for subsequent oxidation and organification. In contrast, FRTL-5 cells are neither polarized nor able to organify iodide. Since the electrochemical gradient for iodide is strongly outward, NIS inhibition will cause net loss from iodide-containing cells, even in the continued presence of extracellular iodide. PFOS did not alter the rate constant for iodide

efflux, suggesting that the decrease in intracellular iodide concentration induced by PFOS is due only to inhibition of NIS-mediated uptake, and not the activation of efflux channels/transporters.

PFOS inhibited iodide accumulation by FRTL-5 cells with an IC_{50} close to 1 μM (log IC_{50} values of -5.99 for the maximal rate of uptake $\Delta[I^-]/\Delta t$, and -6.19 for the concentration of intracellular iodide reached after 10 min of perfusion with NaI), similar to the value obtained for perchlorate in these cells using the same YFP-based assay (Cianchetta et al., 2010). Several small monovalent anions have been shown to inhibit NIS competitively, with an order of potency of PF_6^- > ClO_4^- > BF_4^- > SCN^- >> NO_3^- = ClO_3^- > IO_4^- >> Br^- (Hallinger et al., 2017; Jones et al., 1996; Lecat-Guillet et al., 2007; Tonacchera et al., 2004; Van Sande et al., 2003). Using a high throughput assay, the U.S. EPA's Endocrine Disruptor Screening Program (EDSP) recently demonstrated that PFOS inhibits radioiodide uptake in HEK-293T cells expressing human NIS, but with a more than 10-fold lower potency (log IC_{50} -4.66 to -4.78) (Wang et al., 2019, 2018). In a further study, EDSP reported inhibition of radioiodide uptake in FRTL-5 cells and hNIS-expressing HEK-293T cells by PFOS, with log IC_{50} values of -6.45 and -5.87, respectively (Buckalew et al., 2020). Different potencies may reflect the choice of cell model (heterologous versus endogenous NIS expression), species (human versus rat NIS), detection method (radiotracer versus fluorescent biosensor), and/or other aspects of the experimental protocol (e.g. duration, iodide concentration, and temperature). .

PFOA, in contrast to PFOS, had no effect on iodide uptake by thyroid cells. EDSP also found no effect of PFOA on radioiodide uptake in NIS-expressing HEK-293T cells (Wang et al., 2019). Both compounds belong to the perfluoroalkyl acid class of PFAS that consist of a fluorinated carbon chain of variable length attached to a charged functional group (ITRC, 2018). PFOS ($C_8F_{17}SO_3H$) has 8 perfluorinated carbons and a sulfonic acid head,

whereas PFOA ($C_7F_{15}COOH$) has 7 perfluorinated carbons and a carboxylic acid head (ITRC, 2018). Due to their low pK_a, PFOS and PFOA are almost completely ionized at physiological pH, existing in most biologic matrices as perfluorooctane sulfonate ($C_8F_{17}SO_3^-$) and perfluorooctane caboxylate ($C_7F_{15}CO_2^-$) respectively. It is therefore tempting to speculate that inhibition of iodide uptake by PFOS, but not PFOA, may reflect the activity of the perfluoroalkyl sulfonate but not the carboxylate anion, or may be related to the length of the perfluorinated carbon chain.

The mechanism of NIS inhibition by PFOS is unclear. Indirect effects on cell viability or sodium gradients are unlikely to play a major role, if any, since (i) cytotoxicity was not observed at PFOS concentrations lower than 100 μM, and (ii) the Na-K ATPase inhibitor ouabain only reduced intracellular iodide concentration by 23%, compared to the 82% reduction caused by 10 μM PFOS over the same time frame. Alternatively, inhibition of NIS activity by PFOS may involve direct binding to NIS and/or an interaction with NIS's phospholipid environment. PFAS are known to bind proteins and to partition into phospholipid bilayers, both properties contributing to their bioaccumulation (Ng and Hungerbühler, 2014). Our results indicate that NIS inhibition by PFOS involves reversible single-site binding, suggested by Hill slope estimates close to one, and by the complete restoration of iodide uptake following PFOS washout. Further studies that assess the structure-activity relationship of perfluoroalkyl anions as NIS inhibitors, with reference to the functional group and the length of the fluorocarbon chain, could shed light on the mechanism of NIS inhibition by PFOS.

Small competitive anionic NIS inhibitors, such as perchlorate, thiocyanate and nitrate, are transported by NIS (Portulano et al., 2014), and are concentrated within thyroid follicular cells (Di Bernardo et al., 2011; Wolff, 1964). PFOS is known to be a substrate for other SLC transporters that contribute to its hepatic accumulation, renal clearance and placental

497 transfer (Kummu et al., 2015; Zhao et al., 2017, 2015). Although field and laboratory
498 studies have identified PFAAs in thyroid tissue of several mammalian and non-mammalian
499 species, there is no evidence for active or preferential accumulation in the thyroid gland
500 compared to other tissues (Maestri et al., 2006; Ng and Hungerbühler, 2014). Coperchini
501 et al. (2015) detected PFOS and PFOA in cellular pellets of FRTL-5 thyrocytes grown in
502 the presence of these compounds, and proposed a gradient-based passive diffusion
503 mechanism. In other cell types, PFAA accumulation correlates with phospholipophilicity,
504 suggesting that binding to membrane phospholipids may be the most important factor
505 driving cellular accumulation (Sanchez Garcia et al., 2018). We propose that although
506 PFOS interacts with NIS and/or its environment to inhibit iodide transport, it is not
507 necessarily transported by NIS into cells because of its size or other physicochemical
508 properties.

509 The lowest concentration of PFOS to inhibit iodide uptake in FRTL-5 thyroid cells was 0.3
510 μM (150 ng/ml), a concentration that is only observed in human serum following extreme
511 exposures. PFOS has been detected in the blood of most individuals tested in
512 industrialized nations as a result of occupational, domestic or other accidental exposure.
513 Average serum PFOS levels in the general population are typically <1-30 ng/ml, with
514 maximum individual values occasionally reaching into the 100-1000 ng/ml range (Antonia
515 M Calafat et al., 2007; Antonia M. Calafat et al., 2007; Kannan et al., 2004; Li et al., 2017;
516 Olsen et al., 2003). Thanks to regulatory interventions and voluntary industrial efforts to
517 limit PFAS production, serum PFOS levels in the general population are gradually
518 declining in many countries (Glynn et al., 2012; Kato et al., 2011; Toms et al., 2014).
519 Nevertheless, the widespread use of manufactured goods containing PFAS can result in
520 unexpectedly high exposure levels. High serum PFOS levels (median 345 ng/ml, range
521 24-1500 ng/ml) were detected in people exposed to contaminated municipal drinking

522 water, due to the use fire-fighting foams in a nearby military airfield (Li et al., 2018). In a
523 Canadian family, moderately high levels of serum PFOS (range 15.2−108 ng/ml) were
524 linked to dust ingestion and/or inhalation following home carpet treatment with
525 Scotchguard formulations (Beesoon et al., 2012). Although the present study suggests that
526 PFOS inhibits NIS at concentrations that may be relevant during exceptionally high *in vivo*
527 exposures, an important caveat for the interpretation of the inhibitory concentrations we
528 report, is the absence serum during *in vitro* exposures. It remains to be determined
529 whether binding to serum proteins such as albumin may alter the potency of PFOS as a
530 NIS inhibitor.

531 Epidemiologic and clinical data on the effects of PFAS exposure on thyroid disease risk
532 and thyroid hormone levels are mixed and often inconclusive (reviewed by Coperchini et
533 al., 2017; EFSA, 2018; USEPA, 2016). NHANES studies reported gender-dependent
534 associations of serum PFOS and/or PFOA with treated or subclinical thyroid disease in the
535 US adult population (Melzer et al., 2010; Wen et al., 2013). An association between serum
536 PFAS levels and thyroid disease was also found in exposed chemical plant workers and
537 nearby community residents (Winquist and Steenland, 2014), but not in another population
538 exposed to high PFAS levels through contaminated municipal drinking water (Andersson
539 et al., 2019). PFAS levels show positive/negative, null or ambiguous associations with
540 TSH and thyroid hormone levels in several types of populations including exposed
541 individuals, the general population, pregnant women and mother-infant pairs (Berg et al.,
542 2015; Blake et al., 2018; Inoue et al., 2019; Li et al., 2017; Seo et al., 2018; Tsai et al.,
543 2017). The lack of consensus may reflect differences in study design, population
544 characteristics (size, developmental stage, gender, ethnicity), thyroid status (undiagnosed
545 thyroid disease, iodine sufficiency), and exposure (concentration, duration, mixture
546 effects). In fact, people are exposed to complex mixtures of PFAS present in the

environment, as well as other endocrine disruptors and stressors targeting the HPT axis at different levels. Webster et al. proposed a “multiple hit hypothesis,” postulating that individuals with multiple thyroid stressors (e.g. pregnancy, low iodine, thyroid antibodies), may be more susceptible to PFAS-induced thyroid disruption. (Webster et al., 2016, 2014). Thus, in pregnant women, serum PFAS levels were positively associated with TSH and negatively associated with free T4, but only in women with high levels of thyroid peroxidase antibodies (TPOAb) suggestive of auto-immune thyroid disease (Webster et al., 2014). Furthermore, in the US adult population, associations between serum PFAS and thyroid parameters occurred only those with high TPOAb and low iodine status (Webster et al., 2016). Recent studies have also addressed the combined effects of multiple PFAS in pregnant women, finding either positive or limited associations of PFAS mixtures with thyroid hormones in maternal and cord sera (Lebeaux et al., 2020; Preston et al., 2020).

In vivo studies in rats have shown that PFOS decreases circulating thyroid hormone levels without changing TSH (reviewed in Coperchini et al., 2017). This is contrary to the expected hypothyroid effect of NIS inhibition, such as that induced by perchlorate (Männistö et al., 1979). Several mechanisms for PFOS-induced hypothyroxemia have been proposed, including competitive binding to thyroid hormone transport proteins, increased conversion of thyroxine (T4) to triiodothyronine (T3) by type 1 deiodinase (Yu et al., 2009), and increased hepatic clearance (Coperchini et al., 2017; Yu et al., 2009). Furthermore, our study evaluated acute, but not long-term, effects of PFOS/PFOA on NIS-mediated iodide accumulation in thyroid cells. Chronic PFOS exposure had no effect on NIS mRNA levels in rats (Yu et al., 2009), but increased them in zebrafish larvae (Shi et al., 2009). Further studies to evaluate the long-term effects of PFAS on NIS expression,

localization and function, at concentrations that mirror serum levels, will be critical to extrapolate *in vitro* findings to the interpretation of *in vivo* responses.

5. Conclusion

Although PFAS disruption of thyroid function is still controversial, potential effects may occur through a multitude of mechanisms. Using a cell-based fluorescence assay, we have shown that PFOS inhibits NIS-mediated iodide uptake by thyroid cells *in vitro*. Although inhibition occurs at PFOS concentrations that are unlikely to impact the general population, it may be relevant in susceptible individuals accidentally exposed to exceptionally high levels. Mechanisms other that NIS inhibition may be involved in thyroid disruption by PFOA. Despite the gradual phase-out of PFOS and PFOA from industrial and commercial applications, the widespread use and persistence of PFAS in the human habitat highlights the need for further studies to address the health effects of this important class of anthropogenic chemicals.

6. Acknowledgments

This study was supported by Italy's Ministry of Health grant [RF-2011-02350857] and University of Bologna intramural funds.

7. Author contributions

AC: Data curation; Formal analysis; Investigation; Methodology; Supervision; Writing - review & editing. CS: Investigation; Methodology; Writing - review & editing. KJR: Conceptualization; Data curation; Formal analysis; Funding acquisition; Investigation; Methodology; Project administration; Resources; Supervision; Visualization; Roles/Writing - original draft; Writing - review & editing.

8. References

Ambesi-Impiombato, F.S., Parks, L.A., Coon, H.G., 1980. Culture of hormone-dependent functional epithelial cells from rat thyroids. Proc. Natl. Acad. Sci. U. S. A. 77, 3455–9. https://doi.org/10.1073/pnas.77.6.3455

Andersson, E.M., Scott, K., Xu, Y., Li, Y., Olsson, D.S., Fletcher, T., Jakobsson, K., 2019. High exposure to perfluorinated compounds in drinking water and thyroid disease. A cohort study from Ronneby, Sweden. Environ. Res. 176, 108540. https://doi.org/10.1016/j.envres.2019.108540

Beesoon, S., Genuis, S.J., Benskin, J.P., Martin, J.W., 2012. Exceptionally high serum concentrations of perfluorohexanesulfonate in a Canadian family are linked to home carpet treatment applications. Environ. Sci. Technol. 46, 12960–7. https://doi.org/10.1021/es3034654

Berg, V., Nøst, T.H., Hansen, S., Elverland, A., Veyhe, A.S., Jorde, R., Odland, J.Ø., Sandanger, T.M., 2015. Assessing the relationship between perfluoroalkyl substances, thyroid hormones and binding proteins in pregnant women; a longitudinal mixed effects approach. Environ. Int. 77, 63–69. https://doi.org/10.1016/j.envint.2015.01.007

Blake, B.E., Pinney, S.M., Hines, E.P., Fenton, S.E., Ferguson, K.K., 2018. Associations between longitudinal serum perfluoroalkyl substance (PFAS) levels and measures of thyroid hormone, kidney function, and body mass index in the Fernald Community Cohort. Environ. Pollut. 242, 894–904. https://doi.org/10.1016/j.envpol.2018.07.042

Buckalew, A.R., Wang, J., Murr, A.S., Deisenroth, C., Stewart, W.M., Stoker, T.E., Laws, S.C., 2020. Evaluation of potential sodium-iodide symporter (NIS) inhibitors using a secondary Fischer rat thyroid follicular cell (FRTL-5) radioactive iodide uptake (RAIU)

assay. Arch. Toxicol. 94, 873–885. https://doi.org/10.1007/s00204-020-02664-y

Calafat, Antonia M, Kuklenyik, Z., Reidy, J.A., Caudill, S.P., Tully, J.S., Needham, L.L., 2007. Serum concentrations of 11 polyfluoroalkyl compounds in the u.s. population: data from the national health and nutrition examination survey (NHANES). Environ. Sci. Technol. 41, 2237–42. https://doi.org/10.1021/es062686m

Calafat, Antonia M., Wong, L.Y., Kuklenyik, Z., Reidy, J.A., Needham, L.L., 2007. Polyfluoroalkyl chemicals in the U.S. population: Data from the national health and nutrition examination survey (NHANES) 2003-2004 and comparisons with NHANES 1999-2000. Environ. Health Perspect. 115, 1596–1602. https://doi.org/10.1289/ehp.10598

Cianchetta, S., di Bernardo, J., Romeo, G., Rhoden, K.J., 2010. Perchlorate transport and inhibition of the sodium iodide symporter measured with the yellow fluorescent protein variant YFP-H148Q/I152L. Toxicol. Appl. Pharmacol. 243, 372–380. https://doi.org/10.1016/j.taap.2009.12.004

Coperchini, F., Awwad, O., Rotondi, M., Santini, F., Imbriani, M., Chiovato, L., 2017. Thyroid disruption by perfluorooctane sulfonate (PFOS) and perfluorooctanoate (PFOA). J. Endocrinol. Invest. 40, 105–121. https://doi.org/10.1007/s40618-016-0572-z

Coperchini, F., Pignatti, P., Lacerenza, S., Negri, S., Sideri, R., Testoni, C., de Martinis, L., Cottica, D., Magri, F., Imbriani, M., Rotondi, M., Chiovato, L., 2015. Exposure to perfluorinated compounds: in vitro study on thyroid cells. Environ. Sci. Pollut. Res. 22, 2287–2294. https://doi.org/10.1007/s11356-014-3480-9

Di Bernardo, J., Iosco, C., Rhoden, K.J., 2011. Intracellular anion fluorescence assay for sodium/iodide symporter substrates. Anal. Biochem. 415.

https://doi.org/10.1016/j.ab.2011.04.017

EFSA Panel on Contaminants in the Food Chain (CONTAM), Helle Katrine Knutsen, Jan Alexander, Lars Barreg_ard, Margherita Bignami, B.B., Sandra Ceccatelli, Bruce Cottrill, Michael Dinovi, Lutz Edler, B.G.-K., Christer Hogstrand, Laurentius (Ron) Hoogenboom, Carlo Stefano Nebbia, I.P.O., Annette Petersen, Martin Rose, Alain-Claude Roudot, Christiane Vleminckx, G.V., Heather Wallace, Laurent Bodin, Jean-Pierre Cravedi, T.I.H., Line Sm_astuen Haug, Niklas Johansson, Henk van Loveren, Petra Gergelova, K.M., Sara Levorato, M. van M. and T.S., 2018. Risk to human health related to the presence of perfluorooctane sulfonic acid and perfluorooctanoic acid in food. EFSA J. 16(12), 5194.

Galietta, L.J.V., Haggie, P.M., Verkman, A.S., 2001. Green fluorescent protein-based halide indicators with improved chloride and iodide affinities. FEBS Lett. 499, 220–224. https://doi.org/10.1016/S0014-5793(01)02561-3

Glynn, A., Berger, U., Bignert, A., Ullah, S., Aune, M., Lignell, S., Darnerud, P.O., 2012. Perfluorinated alkyl acids in blood serum from primiparous women in Sweden: serial sampling during pregnancy and nursing, and temporal trends 1996-2010. Environ. Sci. Technol. 46, 9071–9. https://doi.org/10.1021/es301168c

Hallinger, D.R., Murr, A.S., Buckalew, A.R., Simmons, S.O., Stoker, T.E., Laws, S.C., 2017. Development of a screening approach to detect thyroid disrupting chemicals that inhibit the human sodium iodide symporter (NIS). Toxicol. Vitr. 40, 66–78. https://doi.org/10.1016/j.tiv.2016.12.006

Inoue, K., Ritz, B., Andersen, S.L., Ramlau-Hansen, C.H., Høyer, B.B., Bech, B.H., Henriksen, T.B., Bonefeld-Jørgensen, E.C., Olsen, J., Liew, Z., 2019. Perfluoroalkyl substances and maternal thyroid hormones in early pregnancy; findings in the danish

national birth cohort. Environ. Health Perspect. 127, 117002. https://doi.org/10.1289/EHP5482

ITRC (Interstate Technology & Regulatory Council), 2018. PFAS Fact Sheets PFAS-1, Washington, D.C.: Interstate Technology & Regulatory Council, PFAS Team. www.itrcweb.org.

Jones, P.A., Pendlington, R.U., Earl, L.K., Sharma, R.K., Barratt, M.D., 1996. In vitro investigations of the direct effects of complex anions on thyroidal iodide uptake: Identification of novel inhibitors. Toxicol. Vitr. 10, 149–160. https://doi.org/10.1016/0887-2333(95)00114-X

Kannan, K., Corsolini, S., Falandysz, J., Fillmann, G., Kumar, K.S., Loganathan, B.G., Mohd, M.A., Olivero, J., Van Wouwe, N., Yang, J.H., Aldoust, K.M., 2004. Perfluorooctanesulfonate and related fluorochemicals in human blood from several countries. Environ. Sci. Technol. 38, 4489–95. https://doi.org/10.1021/es0493446

Kato, K., Wong, L.Y., Jia, L.T., Kuklenyik, Z., Calafat, A.M., 2011. Trends in exposure to polyfluoroalkyl chemicals in the U.S. Population: 1999-2008. Environ. Sci. Technol. 45, 8037–45. https://doi.org/10.1021/es1043613

KEMI (Swedish Chemicals Agency), 2015. Report 7/15: Occurrence and use of highly fluorinated substances and alternatives, https://www.kemi.se.

Kummu, M., Sieppi, E., Koponen, J., Laatio, L., Vähäkangas, K., Kiviranta, H., Rautio, A., Myllynen, P., 2015. Organic anion transporter 4 (OAT 4) modifies placental transfer of perfluorinated alkyl acids PFOS and PFOA in human placental ex vivo perfusion system. Placenta 36, 1185–91. https://doi.org/10.1016/j.placenta.2015.07.119

Lebeaux, R.M., Doherty, B.T., Gallagher, L.G., Zoeller, R.T., Hoofnagle, A.N., Calafat,

690 A.M., Karagas, M.R., Yolton, K., Chen, A., Lanphear, B.P., Braun, J.M., Romano,
691 M.E., 2020. Maternal serum perfluoroalkyl substance mixtures and thyroid hormone
692 concentrations in maternal and cord sera: The HOME Study. Environ. Res. 185,
693 109395. https://doi.org/10.1016/j.envres.2020.109395

694 Lecat-Guillet, N., Merer, G., Lopez, R., Pourcher, T., Rousseau, B., Ambroise, Y., 2007. A
695 96-well automated radioiodide uptake assay for sodium/iodide symporter inhibitors.
696 Assay Drug Dev. Technol. 5, 535–40. https://doi.org/10.1089/adt.2007.068

697 Li, Y., Cheng, Y., Xie, Z., Zeng, F., 2017. Perfluorinated alkyl substances in serum of the
698 southern Chinese general population and potential impact on thyroid hormones. Sci.
699 Rep. 7, 43380. https://doi.org/10.1038/srep43380

700 Li, Y., Fletcher, T., Mucs, D., Scott, K., Lindh, C.H., Tallving, P., Jakobsson, K., 2018. Half-
701 lives of PFOS, PFHxS and PFOA after end of exposure to contaminated drinking
702 water. Occup. Environ. Med. 75, 46–51. https://doi.org/10.1136/oemed-2017-104651

703 Maestri, L., Negri, S., Ferrari, M., Ghittori, S., Fabris, F., Danesino, P., Imbriani, M., 2006.
704 Determination of perfluorooctanoic acid and perfluorooctanesulfonate in human
705 tissues by liquid chromatography/single quadrupole mass spectrometry. Rapid
706 Commun. Mass Spectrom. 20, 2728–2734. https://doi.org/10.1002/rcm.2661

707 Männistö, P.T., Ranta, T., Leppäluoto, J., 1979. Effects of methylmercaptoimidazole
708 (MMI), propylthiouracil (PTU), potassium perchlorate (KClO4) and potassium iodide
709 (KI) on the serum concentrations of thyrotrophin (TSH) and thyroid hormones in the
710 rat. Acta Endocrinol. (Copenh). 91, 271–81. https://doi.org/10.1530/acta.0.0910271

711 Melzer, D., Rice, N., Depledge, M.H., Henley, W.E., Galloway, T.S., 2010. Association
712 between serum perfluorooctanoic acid (PFOA) and thyroid disease in the U.S.
713 National Health and Nutrition Examination Survey. Environ. Health Perspect. 118,

686–92. https://doi.org/10.1289/ehp.0901584

Ng, C.A., Hungerbühler, K., 2014. Bioaccumulation of Perfluorinated Alkyl Acids: Observations and Models. Environ. Sci. Technol. 48, 4637–4648. https://doi.org/10.1021/es404008g

Olsen, G.W., Burris, J.M., Ehresman, D.J., Froehlich, J.W., Seacat, A.M., Butenhoff, J.L., Zobel, L.R., 2007. Half-life of serum elimination of perfluorooctanesulfonate, perfluorohexanesulfonate, and perfluorooctanoate in retired fluorochemical production workers. Environ. Health Perspect. 115, 1298–305. https://doi.org/10.1289/ehp.10009

Olsen, G.W., Church, T.R., Miller, J.P., Burris, J.M., Hansen, K.J., Lundberg, J.K., Armitage, J.B., Herron, R.M., Medhdizadehkashi, Z., Nobiletti, J.B., O'Neill, E.M., Mandel, J.H., Zobel, L.R., 2003. Perfluorooctanesulfonate and other fluorochemicals in the serum of American Red Cross adult blood donors. Environ. Health Perspect. 111, 1892–1901. https://doi.org/10.1289/ehp.6316

Portulano, C., Paroder-Belenitsky, M., Carrasco, N., 2014. The Na+/I- symporter (NIS): mechanism and medical impact. Endocr. Rev. 35, 106–49. https://doi.org/10.1210/er.2012-1036

Preston, E. V., Webster, T.F., Claus Henn, B., McClean, M.D., Gennings, C., Oken, E., Rifas-Shiman, S.L., Pearce, E.N., Calafat, A.M., Fleisch, A.F., Sagiv, S.K., 2020. Prenatal exposure to per- and polyfluoroalkyl substances and maternal and neonatal thyroid function in the Project Viva Cohort: A mixtures approach. Environ. Int. 139, 105728. https://doi.org/10.1016/j.envint.2020.105728

Rhoden, K.J., Cianchetta, S., Duchi, S., Romeo, G., 2008. Fluorescence quantitation of thyrocyte iodide accumulation with the yellow fluorescent protein variant YFP-H148Q/I152L. Anal. Biochem. 373, 239–246. https://doi.org/10.1016/j.ab.2007.10.020

738 Rhoden, K.J., Cianchetta, S., Stivani, V., Portulano, C., Galietta, L.J. V, Romeo, G., 2007.
739 Cell-based imaging of sodium iodide symporter activity with the yellow fluorescent
740 protein variant YFP-H148Q/I152L. Am. J. Physiol. Cell Physiol. 292, C814-23.
741 https://doi.org/10.1152/ajpcell.00291.2006

742 Sanchez Garcia, D., Sjödin, M., Hellstrandh, M., Norinder, U., Nikiforova, V., Lindberg, J.,
743 Wincent, E., Bergman, Å., Cotgreave, I., Munic Kos, V., 2018. Cellular accumulation
744 and lipid binding of perfluorinated alkylated substances (PFASs) - A comparison with
745 lysosomotropic drugs. Chem. Biol. Interact. 281, 1–10.
746 https://doi.org/10.1016/j.cbi.2017.12.021

747 Seo, S.H., Son, M.H., Choi, S.D., Lee, D.H., Chang, Y.S., 2018. Influence of exposure to
748 perfluoroalkyl substances (PFASs) on the Korean general population: 10-year trend
749 and health effects. Environ. Int. 113, 149–161.
750 https://doi.org/10.1016/j.envint.2018.01.025

751 Shi, X., Liu, C., Wu, G., Zhou, B., 2009. Waterborne exposure to PFOS causes disruption
752 of the hypothalamus-pituitary-thyroid axis in zebrafish larvae. Chemosphere 77,
753 1010–1018. https://doi.org/10.1016/j.chemosphere.2009.07.074

754 Smanik, P.A., Liu, Q., Furminger, T.L., Ryu, K., Xing, S., Mazzaferri, E.L., Jhiang, S.M.,
755 1996. Cloning of the human sodium iodide symporter. Biochem. Biophys. Res.
756 Commun. 226, 339–345. https://doi.org/10.1006/bbrc.1996.1358

757 Tazebay, U.H., Wapnir, I.L., Levy, O., Dohan, O., Zuckier, L.S., Zhao, Q.H., Deng, H.F.,
758 Amenta, P.S., Fineberg, S., Pestell, R.G., Carrasco, N., 2000. The mammary gland
759 iodide transporter is expressed during lactation and in breast cancer. Nat. Med. 6,
760 871–878. https://doi.org/10.1038/78630

761 Toms, L.-M.L., Thompson, J., Rotander, A., Hobson, P., Calafat, A.M., Kato, K., Ye, X.,

762 Broomhall, S., Harden, F., Mueller, J.F., 2014. Decline in perfluorooctane sulfonate
763 and perfluorooctanoate serum concentrations in an Australian population from 2002 to
764 2011. Environ. Int. 71, 74–80. https://doi.org/10.1016/j.envint.2014.05.019

765 Tonacchera, M., Pinchera, A., Dimida, A., Ferrarini, E., Agretti, P., Vitti, P., Santini, F.,
766 Crump, K., Gibbs, J., 2004. Relative potencies and additivity of perchlorate,
767 thiocyanate, nitrate, and iodide on the inhibition of radioactive iodide uptake by the
768 human sodium iodide symporter. Thyroid 14, 1012–9.
769 https://doi.org/10.1089/thy.2004.14.1012

770 Tsai, M.-S., Lin, C.-C., Chen, M.-H., Hsieh, W.-S., Chen, P.-C., 2017. Perfluoroalkyl
771 substances and thyroid hormones in cord blood. Environ. Pollut. 222, 543–548.
772 https://doi.org/10.1016/j.envpol.2016.11.027

773 USEPA (U.S. Environmental Protection Agency), 2016. Drinking Water Health Advisories
774 for PFOA and PFOS (EPA 822-R-16-002/003/004/005) [WWW Document].
775 https://www.epa.gov.

776 Van Sande, J., Massart, C., Beauwens, R., Schoutens, A., Costagliola, S., Dumont, J.E.,
777 Wolff, J., 2003. Anion Selectivity by the Sodium Iodide Symporter. Endocrinology 144,
778 247–252. https://doi.org/10.1210/en.2002-220744

779 Waltz, F., Pillette, L., Ambroise, Y., 2010. A nonradioactive iodide uptake assay for sodium
780 iodide symporter function. Anal. Biochem. 396, 91–95.
781 https://doi.org/10.1016/j.ab.2009.08.038

782 Wang, J., Hallinger, D.R., Murr, A.S., Buckalew, A.R., Lougee, R.R., Richard, A.M., Laws,
783 S.C., Stoker, T.E., 2019. High-throughput screening and chemotype-enrichment
784 analysis of ToxCast phase II chemicals evaluated for human sodium-iodide symporter
785 (NIS) inhibition. Environ. Int. 126, 377–386.

https://doi.org/10.1016/j.envint.2019.02.024

Wang, J., Hallinger, D.R., Murr, A.S., Buckalew, A.R., Simmons, S.O., Laws, S.C., Stoker, T.E., 2018. High-Throughput Screening and Quantitative Chemical Ranking for Sodium-Iodide Symporter Inhibitors in ToxCast Phase I Chemical Library. Environ. Sci. Technol. 52, 5417–5426. https://doi.org/10.1021/acs.est.7b06145

Wang, Z., DeWitt, J.C., Higgins, C.P., Cousins, I.T., 2017. A Never-Ending Story of Per- and Polyfluoroalkyl Substances (PFASs)? Environ. Sci. Technol. 51, 2508–2518. https://doi.org/10.1021/acs.est.6b04806

Webster, G.M., Rauch, S.A., Marie, N.S., Mattman, A., Lanphear, B.P., Venners, S.A., 2016. Cross-Sectional Associations of Serum Perfluoroalkyl Acids and Thyroid Hormones in U.S. Adults: Variation According to TPOAb and Iodine Status (NHANES 2007-2008). Environ. Health Perspect. 124, 935–42. https://doi.org/10.1289/ehp.1409589

Webster, G.M., Venners, S.A., Mattman, A., Martin, J.W., 2014. Associations between Perfluoroalkyl acids (PFASs) and maternal thyroid hormones in early pregnancy: A population-based cohort study. Environ. Res. 133, 338–347. https://doi.org/10.1016/j.envres.2014.06.012

Wen, L.-L., Lin, L.-Y., Su, T.-C., Chen, P.-C., Lin, C.-Y., 2013. Association between serum perfluorinated chemicals and thyroid function in U.S. adults: the National Health and Nutrition Examination Survey 2007-2010. J. Clin. Endocrinol. Metab. 98, E1456-64. https://doi.org/10.1210/jc.2013-1282

WHO (World Health Organization), 2013. State of the science of endocrine disrupting chemicals - 2012 an assessment of the state of the science of endocrine disruptors.

809 Winquist, A., Steenland, K., 2014. Perfluorooctanoic acid exposure and thyroid disease in
810 community and worker cohorts. Epidemiology 25, 255–64.
811 https://doi.org/10.1097/EDE.0000000000000040

812 Wolff, J., 1964. Transport of Iodide and Other Anions in the Thyroid Gland. Physiol. Rev.
813 44, 45–90. https://doi.org/10.1152/physrev.1964.44.1.45

814 Yu, W.-G., Liu, W., Jin, Y.-H., 2009. Effects of perfluorooctane sulfonate on rat thyroid
815 hormone biosynthesis and metabolism. Environ. Toxicol. Chem. 28, 990.
816 https://doi.org/10.1897/08-345.1

817 Yu, W.G., Liu, W., Jin, Y.H., 2009. Effects of perfluorooctane sulfonate on RAT thyroid
818 hormone biosynthesis and metabolism. Environ. Toxicol. Chem. 28, 990–996.
819 https://doi.org/10.1897/08-345.1

820 Zhao, W., Zitzow, J.D., Ehresman, D.J., Chang, S.-C., Butenhoff, J.L., Forster, J.,
821 Hagenbuch, B., 2015. Na+/Taurocholate Cotransporting Polypeptide and Apical
822 Sodium-Dependent Bile Acid Transporter Are Involved in the Disposition of
823 Perfluoroalkyl Sulfonates in Humans and Rats. Toxicol. Sci. 146, 363–73.
824 https://doi.org/10.1093/toxsci/kfv102

825 Zhao, W., Zitzow, J.D., Weaver, Y., Ehresman, D.J., Chang, S.-C., Butenhoff, J.L.,
826 Hagenbuch, B., 2017. Organic Anion Transporting Polypeptides Contribute to the
827 Disposition of Perfluoroalkyl Acids in Humans and Rats. Toxicol. Sci. 156, 84–95.
828 https://doi.org/10.1093/toxsci/kfw236

829

Highlights

- Disruption of thyroid iodide homeostasis by environmental contaminants
- Intracellular iodide in thyroid cells monitored with a fluorescent biosensor
- PFOS inhibits iodide uptake in thyroid cells via the Sodium Iodide Symporter
- PFOS does not stimulate iodide efflux from thyroid cells